Supplementary Information for:

Nucleation of jet engine oil vapours is a large source of aviation-related ultrafine particles

Florian Ungeheuer[1], Lucía Caudillo[1], Florian Ditas[2], Mario Simon[1], Dominik van Pinxteren[3], Dogushan Kilic[4,5], Diana Rose[2], Stefan Jacobi[2], Andreas Kürten[1], Joachim Curtius[1], Alexander L. Vogel[1,*]

[1]Institute for Atmospheric and Environmental Sciences, Goethe-University Frankfurt, Frankfurt am Main, 60438, Germany

[2]Department for Ambient Air Quality, Hessian Agency for Nature Conservation, Environment and Geology, Wiesbaden, 65203, Germany

[3]Atmospheric Chemistry Department (ACD), Leibniz Institute for Tropospheric Research (TROPOS), Leipzig, 04318, Germany

[4]The Department of Earth and Environmental Sciences, the Faculty of Science and Engineering, the University of Manchester, Manchester, UK

[5]National Centre for Atmospheric Science, Manchester, UK

*Correspondence to: vogel@iau.uni-frankfurt.de

This PDF file includes:

Supplementary Note 1.

Jet engine oil constituents

Jet engine oils are mainly composed of only a few constituents selected in terms of their lubricating, cooling and stability characteristics[1]. Base stock materials like pentaerythritol esters or trimethyolpropane esters are combined with organophosphates functioning as anti-wear agents and metal deactivators[2,3]. Amine additives act as antioxidants[4]. In aircraft engines, the oil is circulating and a lubrication oil recovery system ensures the cleaning and reuse of the oil. Although it is a closed system, oil can be released to the atmosphere depending on seal tightness and the venting system[1,5]. These emissions depend on the engine model, the engine design[5] and the operational state[1].

We analysed commonly used oils like the Mobil Jet™ Oil II[6] and Mobil Jet™ Oil 254 (Exxon Mobil, Irving, TX, USA), the Turbo Oil 2197 and 2380 (Eastman, Tennesee, USA) and the AeroShell Turbine Oil 500 (Royal Dutch Shell, The Hague, Netherlands). The composition of these oils can be described in accordance to the safety data sheets mainly by five different compounds: pentaerythritol esters ($C_{27\text{-}38}H_{48\text{-}70}O_8$), trimethylolpropane esters ($C_{27\text{-}34}H_{50\text{-}64}O_6$), N-phenyl-1-naphthylamine ($C_{16}H_{13}N$), alkylated diphenylamine (Bis(4-(1,1,3,3-tetramethylbutyl)phenyl)amine; $C_{28}H_{43}N$) and tricresyl phosphate ($C_{21}H_{21}O_4P$) (Supplementary Figure 1). These compounds have been described as molecular markers for jet engine oil emissions during aircraft operations[7]. We confirmed that finding and, furthermore, detected that trimethylolpropane esters are still in use at Frankfurt International Airport, although it is known that the neurotoxin trimethylolpropane phosphate is formed upon pyrolysis of this oil[8]. Although the safety data sheet of Jet Oil II lists 1,4-Dihydroxyanthraquinone (CAS: 81-64-1), we were not able to detect this compound in either ionization polarity.

Supplementary Note 2.

Error estimation of the jet engine oil UFP mass fraction

We determined the uncertainty of the UFP jet engine oil mass fractions based on calibration-, instrumental- and measurement errors. To ensure a conclusive error calculation we identified several limitations in our analytical process taking them into account by error propagation. For the ambient filter quantification, we used the coefficient of variation of the standard addition of a sample of five pentaerythritol tetrahexanoate calibration curves. We did not consider the calibration errors of the jet oil additives as most of the quantified jet engine oil mass is determined by the group of pentaerythritol- and trimethylolpropane esters with concurrently higher uncertainties (see Supplementary Table 2). Averaging the coefficient of variation and applying it to the average jet engine oil filter- and blank filter mass of each size fraction gave us the absolute error for the

subtractive error propagation yielding the absolute error of the blank correction step. We set the absolute error of each size fraction in ratio to the size respective average blank corrected jet oil mass to obtain the relative errors for the final error propagation. For determination of the ambient UFP mass by SMPS measurements and data integration we considered a relative error of 10%.
In order to determine the error of the Nano-MOUDI characterization we made use of the coefficient of variation of the external pentaerythritol tetrahexanoate calibration and the SMPS measurements standard deviations. We used the average absolute standard deviation of the single SMPS scans during the seven hour experiments of filter collection and blank determination. We calculated the absolute error of the blank corrected SMPS mass per scan by error propagation for each size fraction. Referring these values to the average blank corrected mass per scan yielded the relative error of the SMPS measurements for each size fraction. Combination of the relative error of the SMPS measurements and of the external pentaerythritol tetrahexanoate calibration by error propagation yielded the average relative error for the three size fractions of the Nano-MOUDI characterization. Including the relative errors of the Nano-MOUDI characterization, the ambient SMPS measurements and the ambient filter quantification in a final error propagation step yielded an error of the UFP jet oil mass fraction for the three size ranges. The error analysis follows the equation used to determine the contribution of jet engine oil to the UFP mass giving an error of 52%, 53% and 25% for the 10-18 nm, 18-32 nm and 32-56 nm stage, respectively.

Supplementary Note 3.

UHPLC-HRMS method

Targeted measurements of the jet engine oil constituents in the UFP samples were carried out by using ultra-high performance liquid chromatography (UHPLC) (Vanquish Flex, Thermo Fisher Scientific)/heated electrospray ionization (HESI) combined with an Orbitrap high-resolution mass spectrometer (HRMS) (Q Exactive Focus Hybrid-Quadrupol-Orbitrap, Thermo Fisher Scientific). Chromatographic separation of the jet engine oil constituents was accomplished using a reversed phase column (Accucore C_{18}, 150 x 2.1 mm, 2.6 µm particle size, Thermo Fisher Scientific), thermostated at 40 °C (still air) operated in gradient mode. As mobile phase we used ultrapure water (18.2 MΩ·cm, Millipak® Express 40: 0.22 µm, Millipore; Milli-Q® Reference A+, Merck) with 0.1% formic acid (v/v, solvent A) and methanol (Optima™ LC/MS grade, Fisher scientific) with 0.1% formic acid (v/v, solvent B). Both UHPLC solvents were spiked with formic acid (LiChropur®, Merck, 98-100%) functioning as an acidifier/proton donor. This leads to an enhanced ionization in the positive mode and improves the chromatographic separation.
The total method duration was 20 minutes with a flow rate of 400 µL/min and an injection volume of 5 µL. We started the UHPLC chromatography with 60% solvent B (0-0.5 min). Then we increased solvent B to 90% (0.5-11 min) and then raised up to 99% (11-16 min). In the end, solvent B was

reduced to 60% (16-17 min) to equilibrate the starting conditions for the following measurement within three minutes.

Due to the chemical composition and molecular structure, the jet engine oil constituents form positively charged molecular ions ($[M+H]^+$, $[M+Na]^+$) by adduct formation. Hence, the mass spectrometric detection was conducted by HESI in positive mode. The applied HESI settings were: 350 °C gas temperature, 40 psi sheath gas (nitrogen), 8 psi auxiliary gas (nitrogen) and a spray voltage of 3.5 kV. The measurement for quantification was realised by selected ion monitoring (SIM) with a resolution of ~35k using an inclusion list based on prior measurements of the purchased jet engine oils and ambient samples. At maximum only four compounds were detected simultaneously in a SIM time window to attain highest possible detection sensitivity. Mass spectrometry (MS) data was recorded in profile mode. The target compounds were N-phenyl-1-naphthylamine ($C_{16}H_{13}N$, CAS: 90-30-2), 1,4-Dihydroxyanthraquinone ($C_{14}H_8O_4$, CAS: 81-64-1), tri-*o*-cresyl phosphate ($C_{21}H_{21}O_4P$, CAS: 78-30-8), pentaerythritol esters ($C_{27\text{-}38}H_{48\text{-}70}O_8$), trimethylolpropane esters ($C_{27\text{-}34}H_{50\text{-}64}O_6$) and Bis(4-(2,4,4-trimethylpentan-2-yl)phenyl)amine ($C_{28}H_{43}N$, CAS: 15721-78-5).

Supplementary Note 4.

Quantification method of jet engine oil constituents

Quantification of the jet engine oil constituents was achieved by the use of a standard addition method with authentic standards. For the analysis, we extracted a centred circular punch of the samples with a diameter of 2.5 cm two times, 20 minutes each on a shaker with 100 and 50 µL pure methanol (Optima™ LC/MS grade, Fisher scientific). Glass vials with 200 µL flat bottom micro inserts (LLG Labware, Ø×H: 6×31 mm) were used for the extraction to ensure a covering of the entire filter surface. After the combination of the two extracts, the solvent extracts were then aliquoted onto three glass vials by pipetting 20 µL into 100 µL micro inserts with conical bottoms (VWR, Ø×H: 6×31 mm). One vial was used for the measurement of the native sample and two for the standard addition. The sample extracts were measured directly after extraction. We used pentaerythritol tetrahexanoate (95%, Carbosynth Ltd) for the oil base stock and the oil additives N-phenyl-1-naphthylamine (≥ 98.0%, Sigma-Aldrich), tri-*o*-cresyl phosphate (≥ 97.0%, Sigma-Aldrich), Bis(4-(2,4,4-trimethylpentan-2-yl)phenyl)amine (90%, Fluorochem) and 1,4-Dihydroxyanthraquinone (≥ 98.0%, Sigma-Aldrich). The jet oil base stock is composed of a mixture of pentaerythritol esters with different total carbon chain length of C_{27} – C_{38} attached to the ester groups. As the ionization efficiency of HESI and therefore the resulting signal intensity is mainly dependent on functional groups, we used pentaerythritol tetrahexanoate to quantify all pentaerythritol ester compounds. Standard addition method was chosen to overcome matrix effects because of the strong tendency of the target compounds to adsorb on surfaces.

Two dilutions of the jet engine oil constituents in methanol were prepared, one contained the four additives at 0.08 ng μL^{-1} and pentaerythritol tetrahexanoate at 1.5 ng μL^{-1}. The second dilution was four times higher in concentrations. The concentrations of the different dilutions were set based on single UFP filter measurements and quantification by external calibrations to cover the ambient filter concentration ranges.

After separating the solvent extracts onto three vials 20 µL each, we added 3 µL of each dilution to a respective vial. The degree of dilution of the native sample was adjusted by adding 3 µL of pure methanol. The nominal final concentrations were 0.010 ng μL^{-1} for each additive (N-phenyl-1-naphthylamine, 1,4-Dihydroxyanthraquinone, Bis(4-(2,4,4-trimethylpentan-2-yl)phenyl)amine, tri-*o*-cresyl phosphate) and 0.196 ng μL^{-1} for pentaerythritol tetrahexanoate in the first spiking series and four times higher in the second, respectively. This led to a total of 75 measurements with 3 measurements per UFP filter. Signal integration was automatically carried out by the software Xcalibur (version 4.2.47, Thermo Fisher Scientific), and checked manually. For each compound in every UFP sample a linear regression was accomplished based on the spiked samples allowing to quantify the jet engine oil constituents in the native samples (Supplementary Figure 8). The quantification results were field blank corrected and adjusted with the individual purity of the used calibration standards.

As the ester base stock of trimethylolpropane esters was detected in the course of the data analysis, we used previously measured full scan MS-spectra for quantification of these esters.

Therefore, we applied a correction factor between full-MS and SIM mode of 1.95 that was determined using the surrogate standard pentaerythritol tetrahexanoate.

Supplementary Note 5.

Characterization of the Nano-MOUDI sampler

Various groups used MOUDI and Nano-MOUDI samplers for the collection and subsequent analysis of UFPs[9–12]. However, the quantitative determination is not only challenging because of the very low mass of UFPs (sub-microgram of total particle mass collected after 30-50 hours of sampling), but it is also difficult to account for sampling artefacts while quantifying UFP mass in the Nano-MOUDI sampler. Therefore, we characterized the cascade impactor in the lab using a variety of compounds with different chemical functional groups as surrogates. Finally, we used pentaerythritol tetrahexanoate as representative for jet oil basestocks to attain a loss correction factor for each size distribution stage.

The Nano-MOUDI loss factors were determined based on the quantified filter mass compared to the mass based on the measured particle number size distributions. The loss of particles < 100 nm is dominated by diffusional wall losses[13]. In addition, sampling on the last three Nano-MOUDI stages takes place at reduced pressures down to approximately 1/6 of the ambient pressure

(~17.2 kPa; 18-32 nm stage) and therefore evaporation of semi-volatile compounds is expected to be relevant. In order to determine possible losses of jet engine oil constituents during sampling, we characterized the Nano-MOUDI sampler in a lab experiment by generating nanoparticles of pentaerythritol tetrahexanoate ($C_{29}H_{52}O_8$) and quantification of the collected particle mass. This single ester compound was chosen as a suitable surrogate as the jet engine oils are mainly composed of these synthetic esters. The particle size distribution was measured every 5 min using a scanning-mobility particle sizer (SMPS; D = 2.3-82.2 nm, TSI, model: 3938, Shoreview, MN, USA) containing an electrostatic classifier (EC; TSI, model: 3082) equipped with an Aerosol Neutralizer (TSI, model 3088) and a nano Differential Mobility Analyzer (Nano DMA; TSI, model: 3085A). Particle number concentrations were recorded using an ultrafine condensation particle counter (UCPC; TSI, model: 3776). We used a Constant Output Atomizer (home-built replica of TSI model: 3076) to produce nanoparticles with an average electrical mobility diameter of ~50 nm (Supplementary Figure 9) by using ~0.1 g/L pentaerythritol tetrahexanoate in methanol. The formed nanoparticles pass a diffusion dryer filled with preconditioned silica gel. Subsequently they enter a mixing chamber (Volume ~2.2 L) where mixing with clean air provides the flow rate needed for the analysis. The particles follow the airstream to the Nano-MOUDI for particle collection and to the SMPS system. In order to guarantee a laminar flow (Reynolds number < 2100) the aluminium tube connection between the mixing chamber and the Nano-MOUDI/SMPS system was designed based on the equation to estimate the laminarisation length for a straight tube[14]. At the end of the aluminium tube (ID 1 inch, length 1.5 m) a bend bypass was used to split the flow for the respective analysis. The flow rates were adjusted according to the instruments used, the setup with the detailed flow rates is shown in Supplementary Figure 10.

We collected nanoparticles on the last three Nano-MOUDI stages for 7 hours in triplicate experiments. Two blank measurements with pure methanol were conducted equally to correct for nanoparticle formation from solvent impurities. We determined the deposited mass on each Nano-MOUDI size distribution stage by integration of the particle size number distribution assuming spherical particles and using the pentaerythritol tetrahexanoate density (1.014 g cm^{-3}). The mass of the blank measurements was determined equally using a unit density of 1 g cm^{-3} (Details see Supplementary Table 3). Averaging the blank masses stage wise and subtracting of the corresponding masses provided the corrected mass, based on the measured particle number size distribution. The resulting mass was adjusted with the purity of the used pentaerythritol tetrahexanoate standard. The aluminium filter extraction was conducted as described above. Mass spectrometric analysis was carried out in SIM mode and quantification by external calibration using the pentaerythritol tetrahexanoate standard. We calibrated five points in the range of 0.1-15 ng μL^{-1} and measured each calibration point three times in succession. The calibration function was determined based on the average of the measurements of each concentration. The quantified filter mass was adjusted with the purity of the pentaerythritol tetrahexanoate standard.

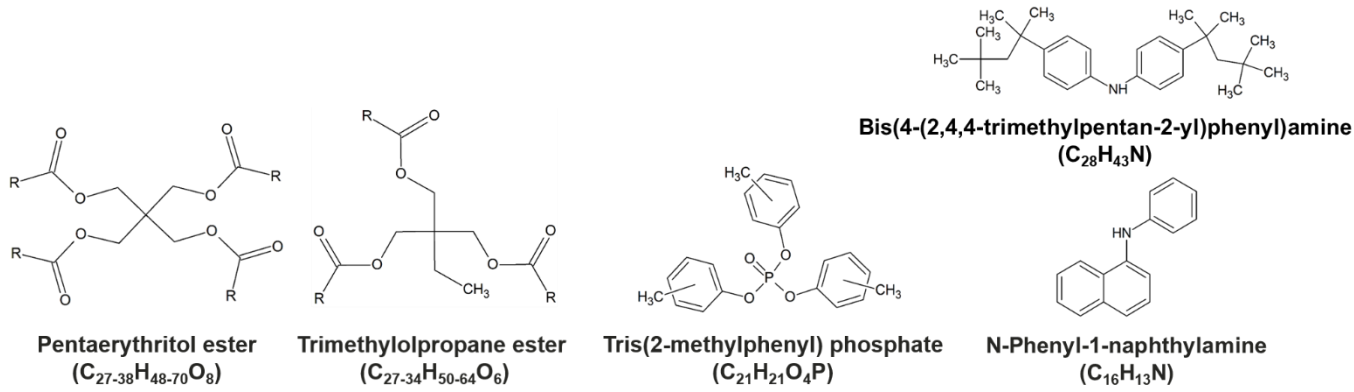

Supplementary Figure 1. Most prominent jet engine lubrication oil constituents.

Supplementary Figure 2. Map showing the sampling site in a distance of 4 km to Frankfurt Airport (www.openstreetmap.org/copyright).

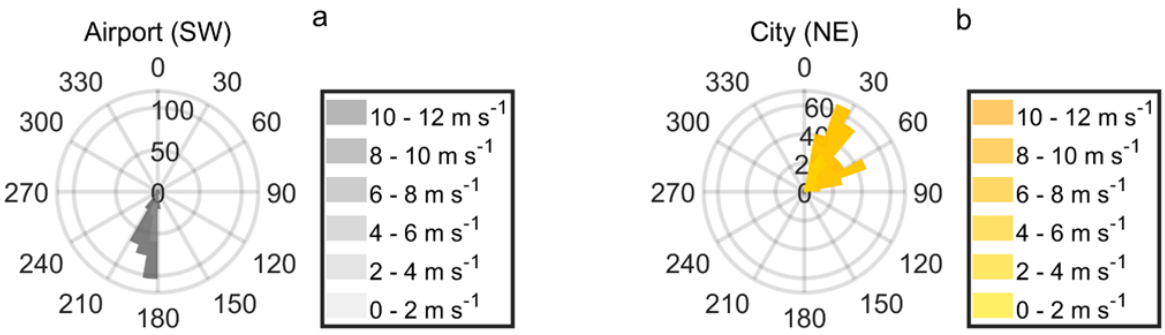

Supplementary Figure 3. Wind roses related to figure 1a showing the wind direction of the ambient SMPS data (Airport (a)- and city (b) direction) averaged over three days (05:00–23:00 CET).

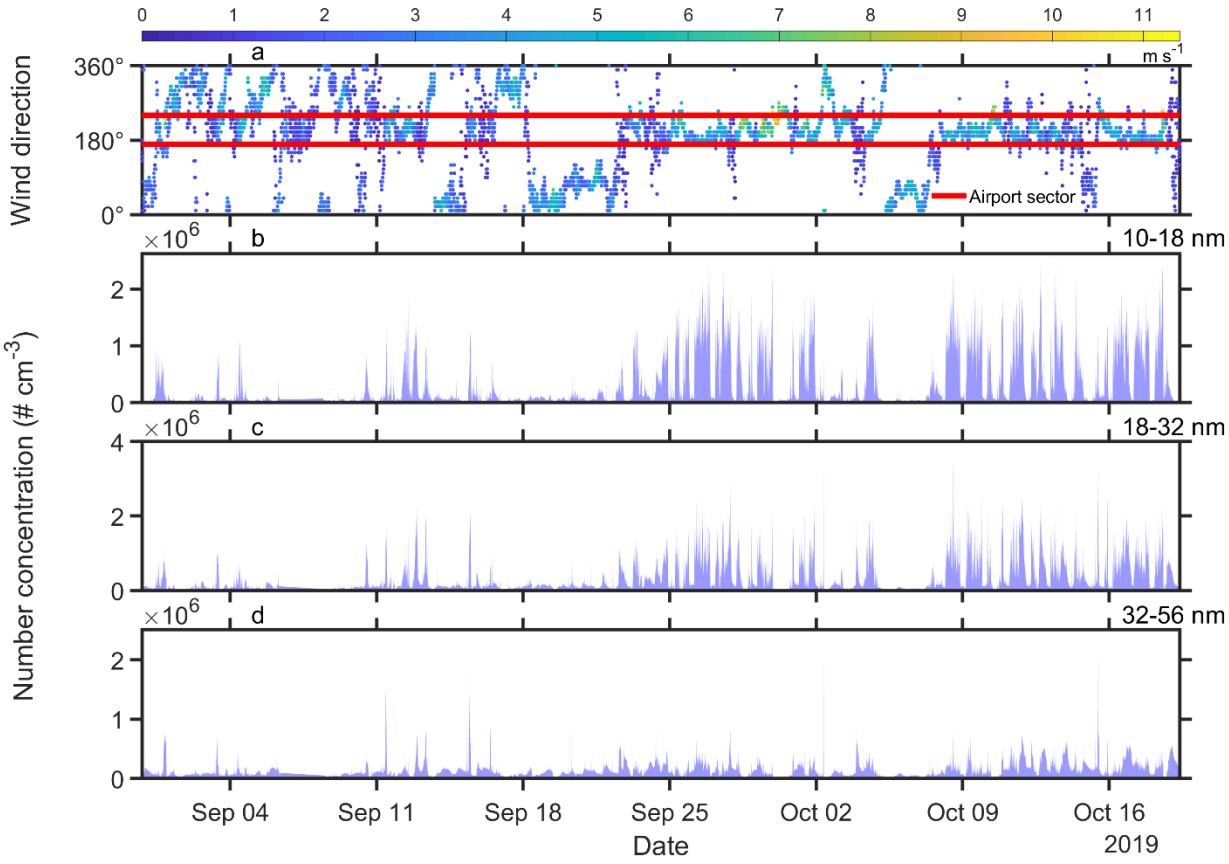

Supplementary Figure 4. Overview of the size-resolved UFP number concentration (# cm^{-3}) measurements at Frankfurt Airport. Wind direction (a) with wind speed indicated by colour bar. The wind data is provided by the meteorological station at Frankfurt Airport (International Civil Aviation Organization, ICAO, code: EDDF) of the German weather service (DWD). The ambient UFP number concentration (# cm^{-3}) in the size ranges (b) 10-18 nm, (c) 18-32 nm and (d) 32-56 nm are shown.

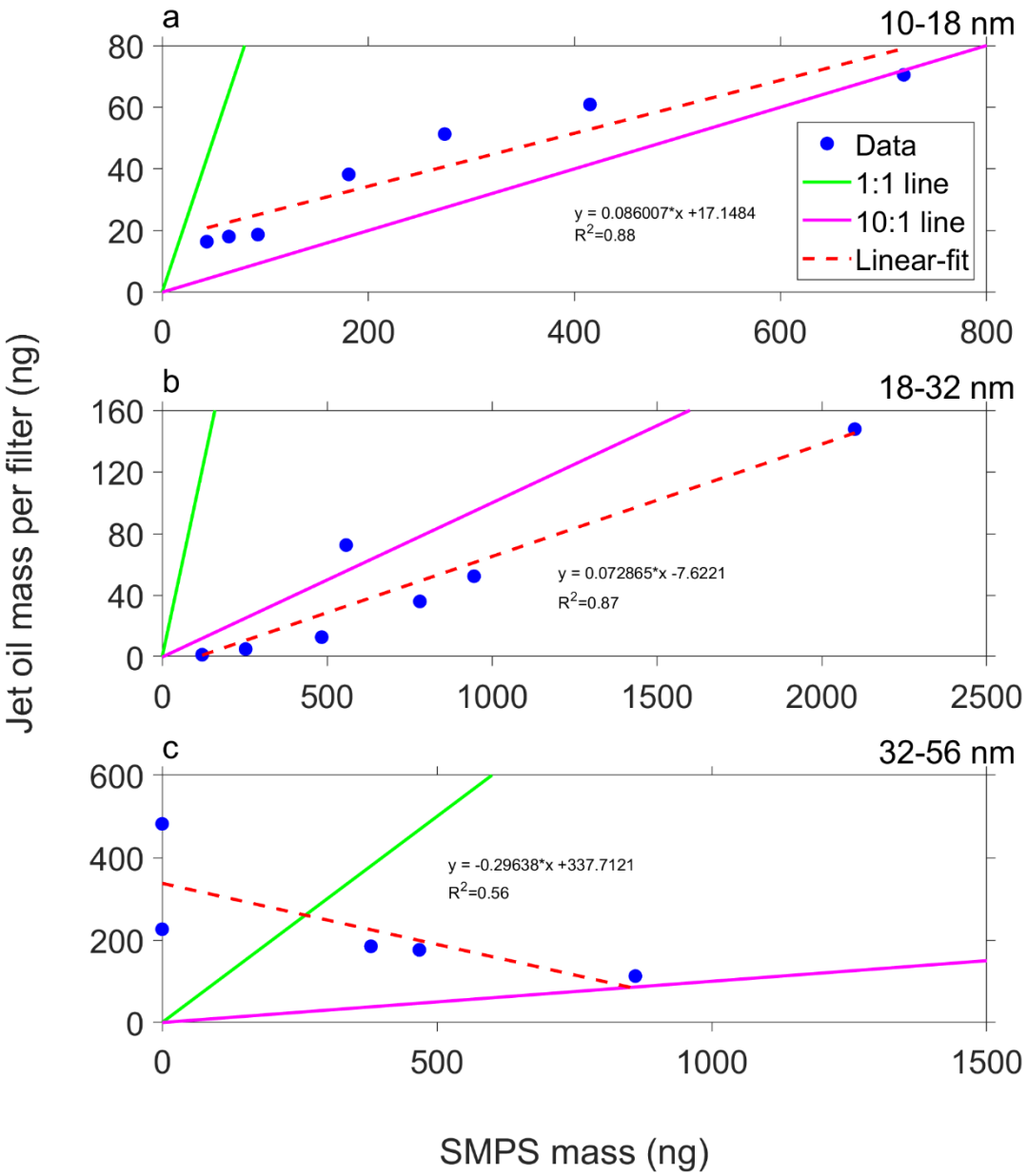

Supplementary Figure 5. Correlation between the corrected jet oil mass per filter and the ambient SMPS mass showing a distinct correlation for the 10-18 nm (a) and 18-32 nm (b) size range. For the 32-56 nm (c) size range no correlation can be observed.

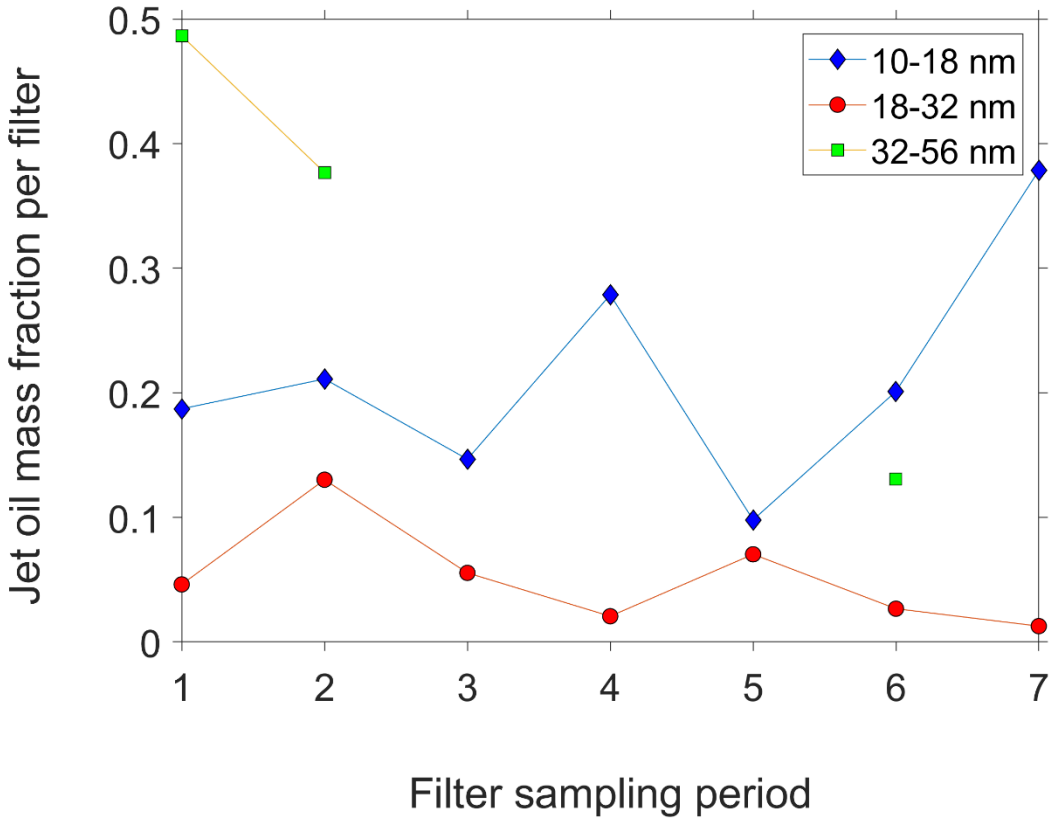

Supplementary Figure 6. Jet oil mass fractions of the collected filter samples for the three Nano-MOUDI size stages (10-18 nm, 18-32 nm, 32-56 nm). The values of the 32-56 nm stage are limited and artificially high due to a high SMPS background correction.

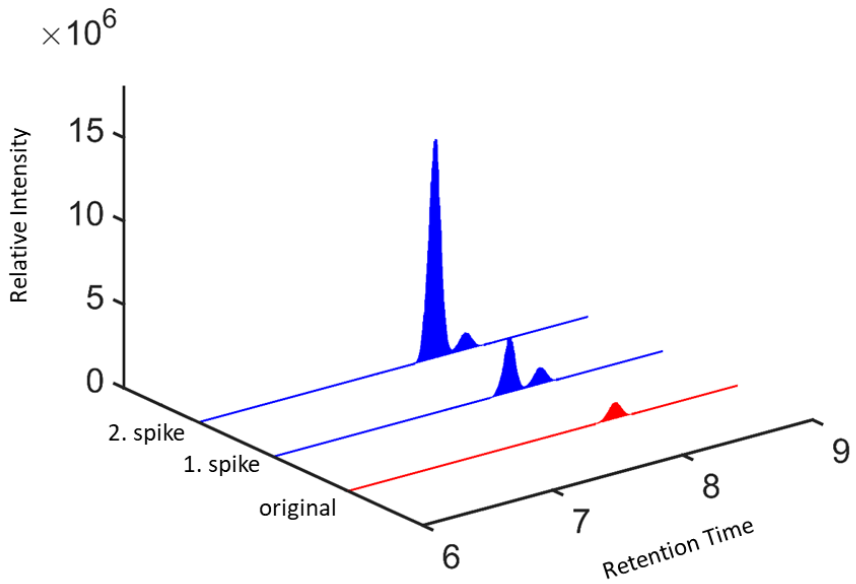

Supplementary Figure 7. Development of the extracted ion chromatogram (XIC) of tricresyl phosphate ([M+Na]$^+$: 391.1069) during the add-on steps. The added tri-*o*-cresyl phosphate ($C_{21}H_{21}O_4P$) forms a peak signal left of the original sample signal, which indicates no high *ortho*-isomer concentrations in the airport samples.

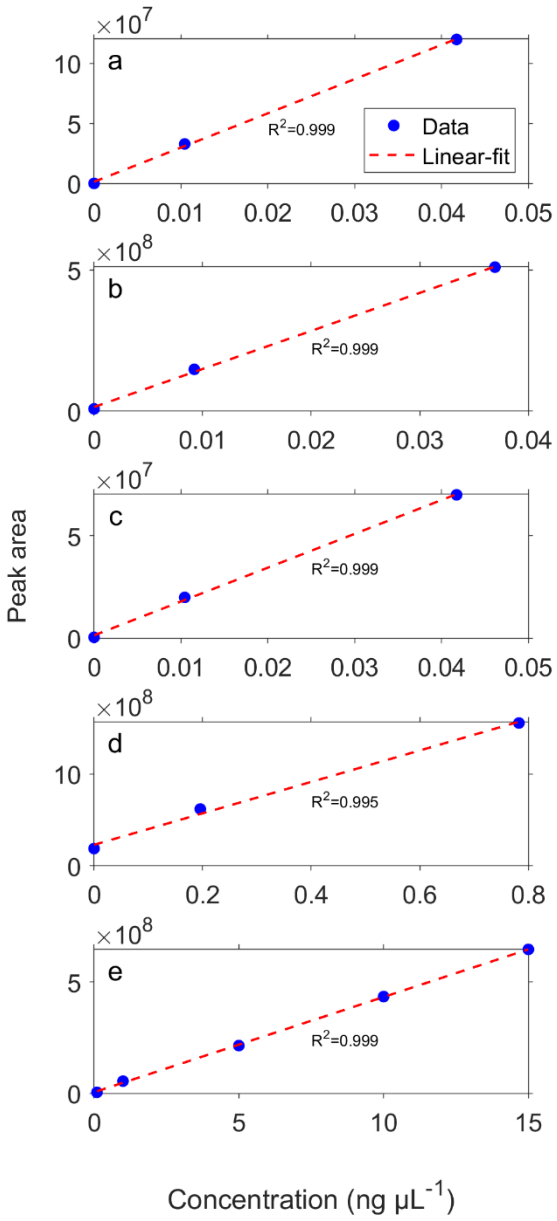

Supplementary Figure 8. Standard addition calibration curves of (a) N-phenyl-1-naphthylamine, (b) alkylated diphenylamine, (c) tricresyl phosphate and (d) pentaerythritol tetrahexanoate. Plot (e) shows the pentaerythritol tetrahexanoate external calibration curve for the Nano-MOUDI characterization.

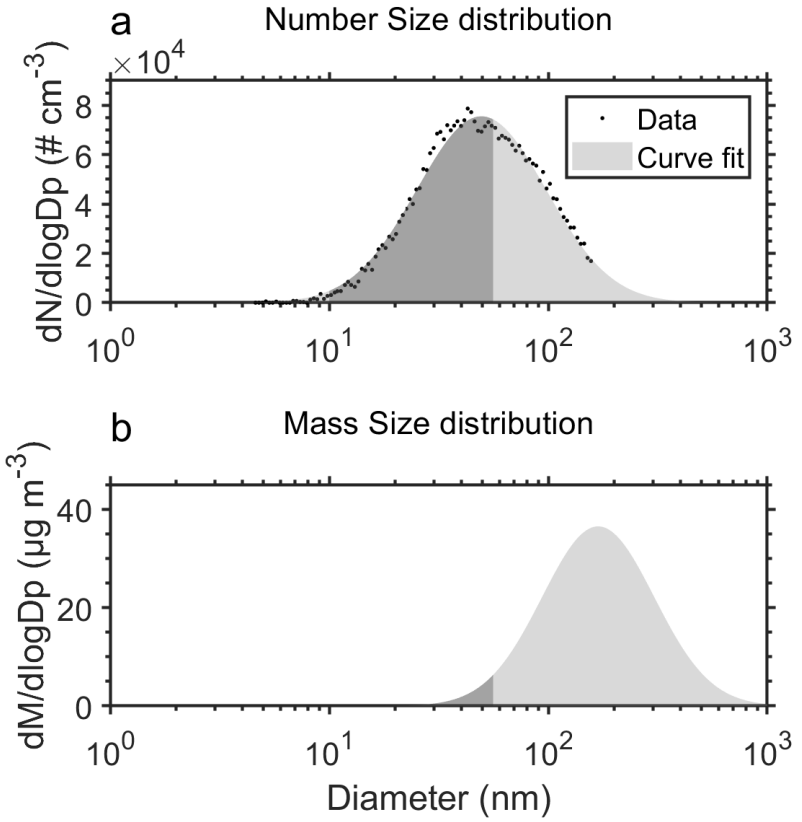

Supplementary Figure 9. Particle number size and mass distribution (a, b) of the pentaerythritol tetrahexanoate nanoparticles formed for the Nano-MOUDI sampler characterization. The dark shading indicates the size range of particle deposition in the Nano-MOUDI stages.

a

b

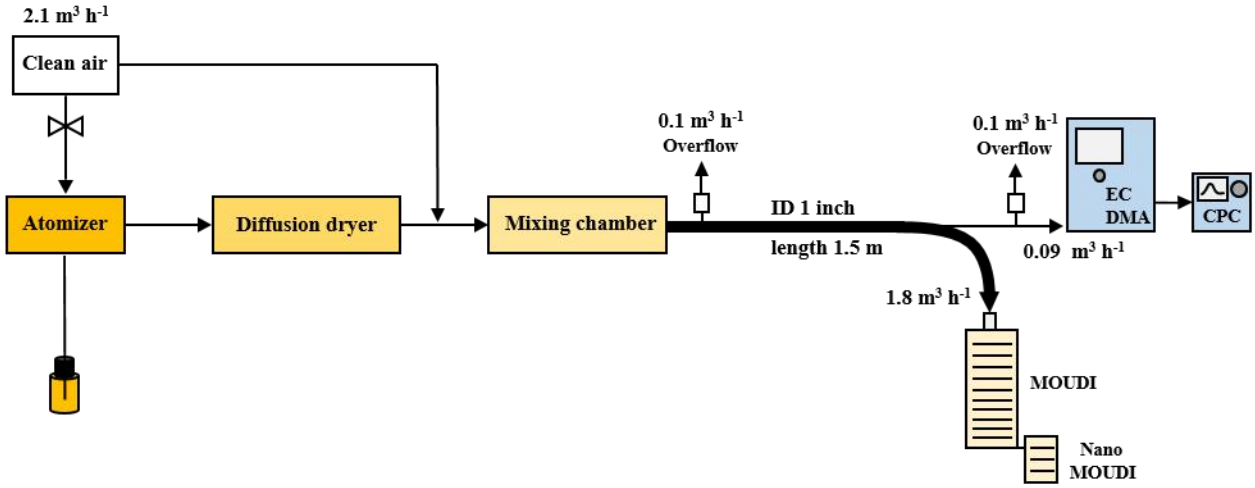

Supplementary Figure 10. (a) Photo of the setup to characterize the Nano-MOUDI regarding possible sampling artefacts and to determine loss factors for the 10-18 nm, 18-32 nm and 32-56 nm size stages. (b) Schematic representation of the Nano-MOUDI characterization setup including the detailed flow rates used.

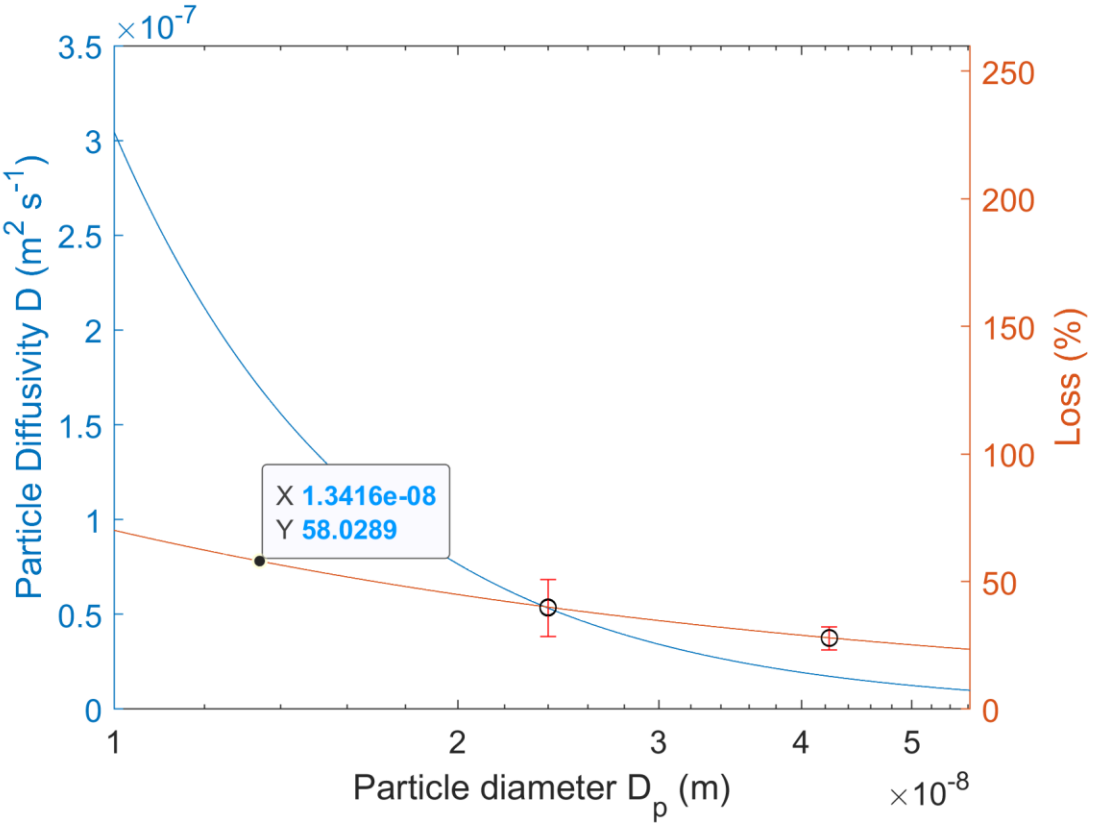

Supplementary Figure 11. Dependency between particle diffusivity, particle diameter and the experimental Nano-MOUDI loss factors. Using an exponential damping term to calculate the particle loss of 58% on the smallest Nano-MOUDI stage (10-18 nm). This term fits the particle loss factors and diffusion coefficients and is based on the particle diffusivity equation.

Supplementary Table 1. UFP mass fractions of jet engine oil with lowest to highest and average contributions for the three Nano-MOUDI size stages.

Particle diameter (nm)	Range of oil contribution to total UFP mass (%)	Average oil contribution to total UFP mass (%)	Average oil contribution to total UFP mass not background corrected (%)
10-18	10 - 38	21 ± 11	18
18-32	1 - 13	5 ± 3	3
32-56	13 - 49*	33* ± 8	9

* These values are artificially high due to a high SMPS background correction in this size range.

Supplementary Table 2. The ambient UFP mass fractions of the single jet engine oil constituents averaged over all size stages are shown. The vapour pressures of the different compounds and compound classes are listed.

Jet oil constituents	$C_{16}H_{13}N$	$C_{21}H_{21}O_4P$	$C_{28}H_{43}N$	$C_{27\text{-}38}H_{48\text{-}70}O_8$	$C_{27\text{-}34}H_{50\text{-}64}O_6$
Ambient constituent fraction (%)	0.10	0.34	0.10	94.87	4.58
Mobil II constituent fraction (measured)	2.15	5.22	1.05	91.57	-
Mobil II constituent fraction (MSDS)	1	1 - < 3	-	-	-
Vapour pressure* (Pa)	3.85E-03	1.45E-05	6.73E-06	3.12E-08***	2.37E-06****
Vapour pressure** (Pa)	8.32E-04	1.53E-07	2.21E-08	1.54E-10 - 2.36E-15	2.43E-09 - 2.10E-12

* Calculated with EPI Suite (25 °C)[15].
** Calculated with SIMPOL.1 (20 °C)[16].
*** Vapour pressure of $C_{29}H_{52}O_8$.
**** Vapour pressure of $C_{27}H_{50}O_6$.

Supplementary Table 3. SMPS masses of the individual Nano-MOUDI characterization experiments. The collected pentaerythritol tetrahexanoate mass was determined using the density of 1.014 g cm^{-3}. For the blank mass a unit density of 1 g cm^{-3} was used.

Collection 1	
Nano MOUDI stage	**Total collected mass [ng]**
32 - 56 nm	2574.0
18 - 32 nm	249.7
10 - 18 nm	8.4
10 - 56 nm	2832.1
Collection 2	
Nano MOUDI stage	**Total collected mass [ng]**
32 - 56 nm	3641.0
18 - 32 nm	368.5
10 - 18 nm	14.5
10 - 56 nm	4024.0
Collection 3	
Nano MOUDI stage	**Total collected mass [ng]**
32 - 56 nm	3643.5
18 - 32 nm	388.4
10 - 18 nm	16.2
10 - 56 nm	4048.1
Blank 1	
Nano MOUDI stage	**Total collected mass [ng]**
32 - 56 nm	974.2
18 - 32 nm	173.7
10 - 18 nm	14.7
10 - 56 nm	1162.6
Blank 2	
Nano MOUDI stage	**Total collected mass [ng]**
32 - 56 nm	1245.1
18 - 32 nm	215.4
10 - 18 nm	14.3
10 - 56 nm	1474.9

Supplementary References

1. Yu, Z. *et al.* Characterization of lubrication oil emissions from aircraft engines. *Environ. Sci. Technol.* **44,** 9530–9534; 10.1021/es102145z (2010).
2. Wyman, J. F., Porvaznik, M., Serve, P., Hobson, D. & Uddin, D. E. High Temperature Decomposition of Military Specification L-23699 Synthetic Aircraft Lubricants. *J. Fire Sci.* **5,** 162–177; 10.1177/073490418700500303 (1987).
3. Du Han, H. & Masuko, M. Elucidation of the Antiwear Performance of Several Organic Phosphates Used with Different Polyol Ester Base Oils from the Aspect of Interaction between Additive and Base Oil. *Tribol. T.* **41,** 600–604; 10.1080/10402009808983788 (1998).
4. Wu, Y., Li, W., Zhang, M. & Wang, X. Improvement of oxidative stability of trimethylolpropane trioleate lubricant. *Thermochim. Acta* **569,** 112–118; 10.1016/j.tca.2013.05.033 (2013).
5. Timko, M. T. *et al.* Composition and Sources of the Organic Particle Emissions from Aircraft Engines. *Aerosol Sci. Technol.* **48,** 61–73; 10.1080/02786826.2013.857758 (2014).
6. Winder, C. & Balouet, J.-C. The toxicity of commercial jet oils. *Environ. Res.* **89,** 146–164; 10.1006/enrs.2002.4346 (2002).
7. Fushimi, A., Saitoh, K., Fujitani, Y. & Takegawa, N. Identification of jet lubrication oil as a major component of aircraft exhaust nanoparticles. *Atmos. Chem. Phys.* **19,** 6389–6399; 10.5194/acp-19-6389-2019 (2019).
8. Ungeheuer, F., van Pinxteren, D. & Vogel, A. L. Identification and source attribution of organic compounds in ultrafine particles near Frankfurt International Airport. *Atmos. Chem. Phys.* **21,** 3763–3775; 10.5194/acp-21-3763-2021 (2021).
9. Díaz-Robles, L. A. *et al.* Health risks caused by short term exposure to ultrafine particles generated by residential wood combustion: a case study of Temuco, Chile. *Environ. Int.* **66,** 174–181; 10.1016/j.envint.2014.01.017 (2014).
10. Andrade-Oliva, M.-A. *et al.* In vitro exposure to ambient fine and ultrafine particles alters dopamine uptake and release, and D2 receptor affinity and signaling. *Environ. Toxicol. Pharmacol.* **80,** 103484; 10.1016/j.etap.2020.103484 (2020).
11. Focsa, C. *et al.* Multi-technique physico-chemical characterization of particles generated by a gasoline engine: Towards measuring tailpipe emissions below 23 nm. *Atmos. Environ.* **235,** 117642; 10.1016/j.atmosenv.2020.117642 (2020).
12. Takegawa, N. *et al.* Characteristics of sub-10 nm particle emissions from in-use commercial aircraft observed at Narita International Airport. *Atmos. Chem. Phys.* **21,** 1085–1104; 10.5194/acp-21-1085-2021 (2021).
13. Weiden, S.-L. von der, Drewnick, F. & Borrmann, S. Particle Loss Calculator – a new software tool for the assessment of the performance of aerosol inlet systems. *Atmos. Meas. Tech.* **2,** 479–494; 10.5194/amt-2-479-2009 (2009).

14. Bird, R. B., Stewart, W. E. & Lightfoot, E. N. *Transport phenomena.* 2nd ed. (Wiley, New York, 2007).
15. United States Environmental Protection Agency. *US EPA. [2021]. Estimation Programs Interface Suite™ v 4.11* (Washington, DC, USA,).
16. Pankow, J. F. & Asher, W. E. SIMPOL.1: a simple group contribution method for predicting vapor pressures and enthalpies of vaporization of multifunctional organic compounds. *Atmos. Chem. Phys.* **8,** 2773–2796; 10.5194/acp-8-2773-2008 (2008).